(Received 25 June 2024, Accepted 20 September 2024, Scheduled 5 October 2024)

Human Identification Using Near-Field Bi-Static Radar at Low Frequencies

Nicole Tan Xin Hui[1*], Ng Oon-Ee[2], Gobi Vetharatnam[1], Teoh Chin Soon[3], and Grant Ellis[4]

[1]*LKC Faculty of Engineering Science, Universiti Tunku Abdul Rahman, Sungai Long Campus, 43000 Kajang, Selangor, Malaysia*
[2]*School of Engineering, Faculty of Technology and Innovation, Taylor's University, 47500 Subang Jaya, Selangor, Malaysia*
[3]*DreamCore Technologies Sdn Bhd, 303-4-5 and 303-4-6, Block B, Krystal Point Jalan Sultan Azlan Shah, 11900 Sungai Nibong, Penang, Malaysia*
[4]*An Independent Researcher, Penang, Malaysia*

ABSTRACT: Near-field scattering of human targets in the view of a bi-static, radar-like sensor operating in the lower radiofrequencies is used as an alternative to traditional biometric identification systems. These radiofrequency-based human sensor systems have emerged as a promising solution to address privacy concerns, particularly those associated with audio and visual data that extract sensitive personally identifiable information. In this paper, we propose a novel method for privacy-preserving human identification using bi-static radar-like sensors. Unlike conventional radar systems that rely on echoes and reflections in the far field, our approach is based on the transmission of signals through and around users as they pass through a transmitter and receiver. Instead of the more commonly used linear or segmented swept frequencies, this work utilizes discrete swept frequencies to transmit and receive radiofrequency signals. We have examined the performance of seven machine learning models in terms of accuracy and processing time and found that the Extra Trees ensemble model produced the best results, with an accuracy rate of 94.25% for a sample size of 31 individuals using an Intel(R) Core(TM) i5-10300H CPU @ 2.50 GHz processor.

1. INTRODUCTION

Radiofrequency-based human sensor systems are an active area of research. The rise in popularity of these systems is contributed by the concerns surrounding the privacy of existing biometric systems. This is especially so for audio and vision-based systems as they capture sensitive personally identifiable information such as facial features and voiceprints. Radiofrequency-based systems provide an alternative by leveraging their ability to utilize noninvasive biometric markers such as gait, velocity, heartrate, or respiration.

While most state-of-the-art radiofrequency identification (RFID) systems have a setup akin to mono-static radar with the transmitter and receiver on the same plane, works such as [1] have shown the bi-static setup to be just as, if not more efficient. In this work, we present our novel method of privacy-preserving human identification using the bi-static approach. However, unlike conventional radar systems which rely on echoes and reflections [2], our approach focuses on near-field scattering of users as they walk through the receiver and transmitter antenna pair. The mode of signal transmission in our method differs from radar systems which typically employ linear frequency sweep across a predefined frequency range. Our proposed method utilizes a discrete frequency sweep to extract information from the resonance of wavelengths interacting with different parts of the human body.

The operating principles of our proposed method of human sensing is different from passive RFID systems which utilize an array of spatially separated tags to provide temporal and spatial information. In contrast, we obtain spatial information through the phase and magnitude data collected from the discrete frequency sweep performed.

While the trend in human identification currently leans toward deep learning, through our comparison of various machine learning models we have shown that ensemble machine learning models work best for our set of data in terms of accuracy and time efficiency.

Our contribution in this paper is as follows:

- We demonstrate the potential for a novel human identification system using a bi-static radar-like sensor, with signals generated from a discrete frequency sweep.
- We examine the effects of the type of signal used (magnitude data, phase data, and the combination of both), effect of number of frequencies used, and the effect of sample size on the performance of our system.
- We evaluate the performances of our system using 7 machine learning algorithms (k-nearest neighbour, support vector machine, extra trees, random forest, convolutional neural network (CNN), recurrent neural network (RNN), CNN-RNN) in the context of human identification, focusing on their accuracy and effectiveness in distinguishing between individual persons.

* Corresponding author: Nicole Tan Xin Hui (tan.nicole@1utar.my).

The paper is organised as follows. Section 2 summarises the literature reviewed. The data processing techniques and setup of the system are elaborated in Section 3. Section 4 presents the results and discussion, and Section 5 concludes this paper.

2. RELATED WORK

Radar-based human identification systems typically involve a participant walking toward the radar sensor located at the end of the measured walking path [2–5]. Ref. [6] differs slightly in setup where the radar is located overhead on the doorframe. These frequency modulated carrier wave (FMCW) systems functions are based on echoes and reflections from a person's body as the person walks toward the sensor. This utilizes the range Fourier Transform (range-FFT) principle and Doppler Fourier Transform (Doppler-FFT) and therefore require linear swept frequency transmission which enhances the radar system's sensitivity to changes in the target range. These systems typically process data as time-frequency spectrograms (2-dimensional images).

Another popular human sensing method utilizes WiFi signals. There are two setup configurations used in state-of-the-art work. One involves a WiFi transmitter and receiver arranged in the same plane, facing the same direction, and the participant is required to walk toward the transmitter or receiver [7]. The other setup involves a WiFi transmitter and WiFi receiver arranged a few feet apart from each other and function as a virtual WiFi gate whereby the participant is required to walk on the path between them [8, 9]. Authors of [8] emphasise that the latter orientation is able to provide directional information as opposed to the more popular former orientation. Data collected in these WiFi systems are either in the form of Channel State Information (CSI) or Received Signal Strength Indicator (RSSI), with CSI being a more popular choice. As suggested by [10], it offers more fine-grained information than RSSI which does not include phase information.

Passive RFID setups are typically arranged in a bi-static-like setup with a reader on one side and an array of RFID tags on the other, functioning essentially like an RFID gate [11]. Although the general idea of a setup with a receiver and transmitter positioned across each other with a fixed distance between them is reminiscent of what we are proposing, the operating principles are different. The array of tags provides temporal and spatial information as the participants walk on the path between the reader and array of tags. We obtain spatial information through the discrete swept frequencies.

The general trend of machine learning models in state-of-the-art work lean toward deep learning models such as CNN, RNN, long-short term memory (LSTM), or a combination of them. Researchers favour these models due to their ability to perform automatic feature extraction. However, some researchers have found that manual feature extraction can produce a classifier that is capable of outperforming CNNs. Ref. [6] applied principal component analysis (PCA) to aid in dimensionality reduction and feature extraction. The authors then compared the performances of several machine learning algorithms: support vector machine (SVM), logistic regression, k-nearest neighbor (KNN), random forest and CNN, and found that the random forest model performed the best.

In this paper, we perform a comparison among 7 machine learning models to examine the effects of different machine learning models on tabular data: K-nearest neighbor (KNN), support vector machine (SVM), random forest, extra trees, convolutional neural network (CNN), recurrent neural network (RNN), and a combination of CNN-RNN. CNN, RNN, and CNN-RNN models were selected as they have been widely used in this area of study, while KNN and SVM are standard models used for comparison in related work, but have typically shown to produce poorer results.

While the use of extra trees is rarely found in related literature, we have included them in this work due to their similar structure to random forests which have shown to perform well on similar applications [6, 12]. Outside the area of human identification using microwave signals, a study by [13] on solar radiation showed that extra trees were capable of producing results on par with random forest models.

3. METHODOLOGY

3.1. Setup of System

The system comprises an antenna pair (one transmitter and one receiver), a radio transmitter, radio receiver, and data processor as illustrated in Figure 1 and shown in Figure 2 see [14]. The antennas used here are vertical dipoles, with reflectors fabricated using aluminium sheets. They stand at 180 cm in height

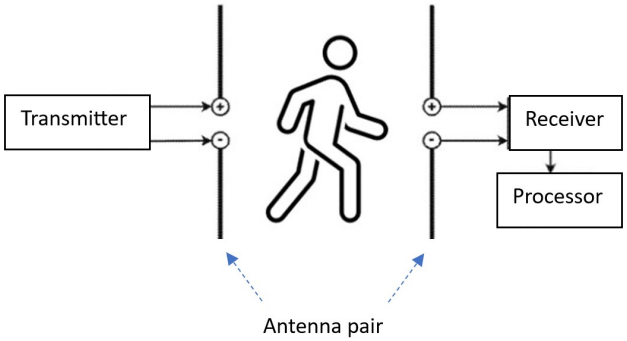

FIGURE 1. Identification system setup.

FIGURE 2. Experimental system configuration including vector network analyser (VNA).

and 15 cm in width, held up by wooden frames. These dipole antennas are arranged 80 cm apart from each other. A ZVL13 Rohde and Schwarz vector network analyser (VNA) is used to synchronise the transmission and reception of discrete frequencies simultaneously. Twelve frequencies were selected in the range of 50 MHz to 920 MHz, which are listed in Table 1 alongside their respective wavelengths. These frequencies were chosen by their ability to capture more significant information from the signals. This was experimentally determined by choosing the measured signals with the greatest variation.

TABLE 1. Frequencies used and their wavelengths.

	Frequencies (MHz)	Wavelength (m)
Freq 1	50	5.996
Freq 2	100	2.998
Freq 3	130	2.306
Freq 4	250	1.199
Freq 5	320	0.937
Freq 6	440	0.681
Freq 7	490	0.612
Freq 8	530	0.566
Freq 9	560	0.535
Freq 10	700	0.428
Freq 11	820	0.366
Freq 12	920	0.326

These frequencies correspond to transmitting power levels between 1 nW and 20 mW (−60 dBm to +13 dBm). Therefore, the maximum power density equates to 0.0009947 mW/cm^2 which is within the threshold of 0.613 mW/cm^2 set by Federal Communications Commission (FCC) [15].

When a person walks between the transmitter-receiver antennas, the signal transmission between them will be modulated by the presence and movement of the person. This information is captured by way of the change in magnitude and phase of the received signal. Shorter wavelengths corresponding to higher frequencies tend to resonate with smaller body parts, such as the arms and legs, whereas larger wavelengths corresponding to lower frequencies resonate with the entire length of the body [16]. Having data from more frequencies selected in the segmented sweep would provide more information; however, this would result in a slower sampling rate. Therefore, in order to optimize the performance of the VNA, 12 frequencies were selected. These frequencies (Table 1) were determined experimentally to produce more significant variation than ambient readings.

3.2. Dataset

Data from 31 individuals have been measured and collected in an open indoor setting. The dataset collected consists of 16 females and 15 males in the age range of 19 to 49. A summary of their physical attributes is tabulated in Table 2. The identities of participants have been concealed to ensure anonymity.

Each individual was required to walk in a straight line between the two antenna sensors as marked out by the yellow arrow in Figure 2. This walking path is 360 cm in length: 180 cm before the antennas and 180 cm after the antennas. In order to replicate real-life scenarios and generate a more robust identification system, three walking conditions were employed: regular walking without electronic devices or additional load, walking while carrying electronic devices without a bag, and walking while carrying electronic devices and a bag. Each walking event was repeated five times, resulting in a total of 15 measurements per participant across all walking conditions. Participants were instructed to maintain a consistent walking pace throughout the experiment. These measurements were repeated 15 times for each individual with no sudden movements or significant changes in their speed. The signal data collected are in the form of phase and magnitude data from the forward transmission coefficient from input port 1 to output port 2.

TABLE 2. Summary of participant details

No.	Age	Gender (M/F)	Height (cm)	Weight (kg)
1	24	M	170	110
2	23	M	172	62
3	23	M	166	48
4	19	F	154.5	43
5	19	F	163	52
6	22	F	160	47
7	23	F	153	50
8	19	F	160	68
9	40	M	168	62
10	39	M	180	80
11	36	F	168	65
12	41	F	160	53
13	49	F	158	73
14	28	M	170	72
15	24	M	174	70
16	23	F	163	46
17	23	M	171	54
18	28	F	170	68
19	41	F	163	68
20	24	F	170	63
21	25	F	159	52
22	24	F	169	49.2
23	23	M	173	60
24	23	F	163	54
25	22	M	177	75
26	22	M	170	58
27	23	F	159	49
28	23	M	165	71
29	23	M	173	76
30	23	M	182	80
31	23	M	169	60

3.3. Classification

The collected data was normalised for the data sets for all 31 individuals. Each measured value was divided with the corresponding ambient magnitude and phase values measured with no one present. The corresponding class labels were generated for each set of data to aid in the supervised learning process. The 10-fold cross validation technique was applied to each classifier with data split into: 80% as training data and 20% as validation data. These normalised values were then used as the input to the 7 machine learning models as mentioned previously in Section 2.

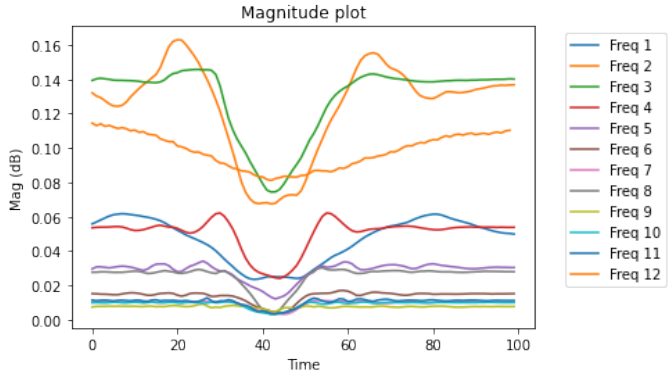

FIGURE 3. Sample of magnitude data.

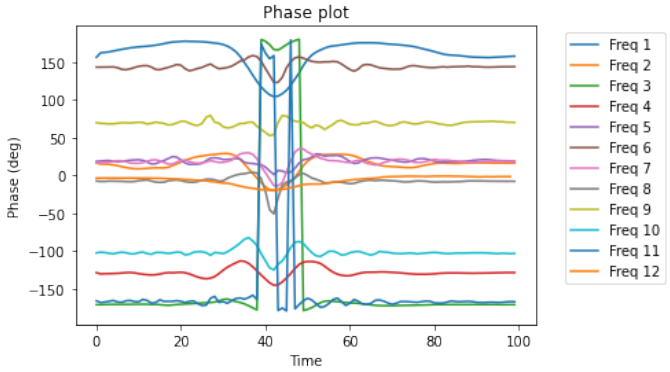

FIGURE 4. Sample of phase data.

4. RESULTS AND DISCUSSION

4.1. Analysis of Captured Data

Samples of captured signals are as shown in Figure 3 and Figure 4, each depicting magnitude and phase data respectively.

The different colours represent signal data from each of the 12 discrete swept frequencies. As can be observed in Figure 4, we face an issue of phase wrapping. This was addressed using the method of phase unwrapping by [12]. The outcome after phase unwrapping at these twelve frequencies is shown in their individual phase plots in Figure 5 to facilitate easier viewing.

The effect of the claim by [16] can be observed in Figure 5, whereby the oscillating effect becomes more pronounced as the frequency increases. The signals in the range of 320 MHz to 920 MHz, labelled as "Freq_5" to "Freq_12", show oscillating effects, which we can infer to be from the resonance of shorter wavelengths and moving limbs. In contrast, the lower frequencies in the range of 50 MHz to 250 MHz, labelled as "Freq_1" to "Freq_4", do not exhibit such pronounced oscillations and therefore can be inferred to be the resonance of longer wavelengths with a larger body part such as the torso.

In our investigation, we conducted feature extraction to identify the minimum points associated with each frequency. As depicted in Figure 6, the resulting features exhibit notable clustering patterns among individuals, with certain frequencies such as "Freq_2", "Freq_3", "Freq_4", "Freq_5", "Freq_12", and "Freq_12" exhibiting clearer distinctions than others. This observation underscores the capability of discrete frequencies to capture individual-specific information, thereby holding promise for potential applications in identification tasks. Our findings show the prospect of leveraging feature extraction methodologies for future research endeavors.

4.2. Comparison of Collected Parameters

We explored the influence of utilizing magnitude-only, phase-only, and a combination of magnitude and phase data on classification accuracy. Our findings, depicted in Figure 7, reveal that phase-only data contributes to a higher accuracy rate at 85.25% than using magnitude-only data at 80.43%. We can infer that phase information is more descriptive than magnitude data as stated by [13]. The combination of magnitude and phase data produces optimum results at 94.25%. This evaluation was performed using a random forest machine learning model.

Next, we examined the effect of increasing number of frequencies. Figure 8 illustrates a consistent pattern of accuracy improvement. This increment is more pronounced when the number of frequencies increases from 1 to 4, whereas the accuracy rates reach a plateau, progressing by approximately less than 1% per step as it increases from 5 frequencies to 12. This observation may be attributed to the feature importance of each frequency as illustrated in Figure 9, whereby frequencies 1 to 3 (labelled as "Freq_1", "Freq_2" and "Freq_3") have a higher score of feature importance than the subsequent frequencies.

4.3. Effect of Group Size

It can be observed from Figure 10 that accuracy decreases with the increase in group size. We have examined the correlation between sample size and accuracy in our work and found a strong negative correlation coefficient between the two at -0.99345. We have further examined this correlation among related works [2, 7, 8, 11, 12] as summarised in Table 3 and found that the same trend applies. This suggests that as sample size increases, the variability within the data also increases, making it more challenging for the model to maintain the same level of accuracy. Therefore, ideal systems should be able to achieve high levels of accuracy even in large sample size.

TABLE 3. Correlation coefficient between sample size and accuracy among related work.

System	Correlation coefficient
mID [2]	-0.96686
Wihi [7]	-0.972761
Gate-ID [8]	-0.959847
RFree-ID [11]	-0.995823
RFPass [12]	-0.985801
Ours	-0.99345

4.4. Comparison of Machine Learning Models

We have evaluated the performance of seven machine learning models mentioned in Subsection 3.3. The results are as shown

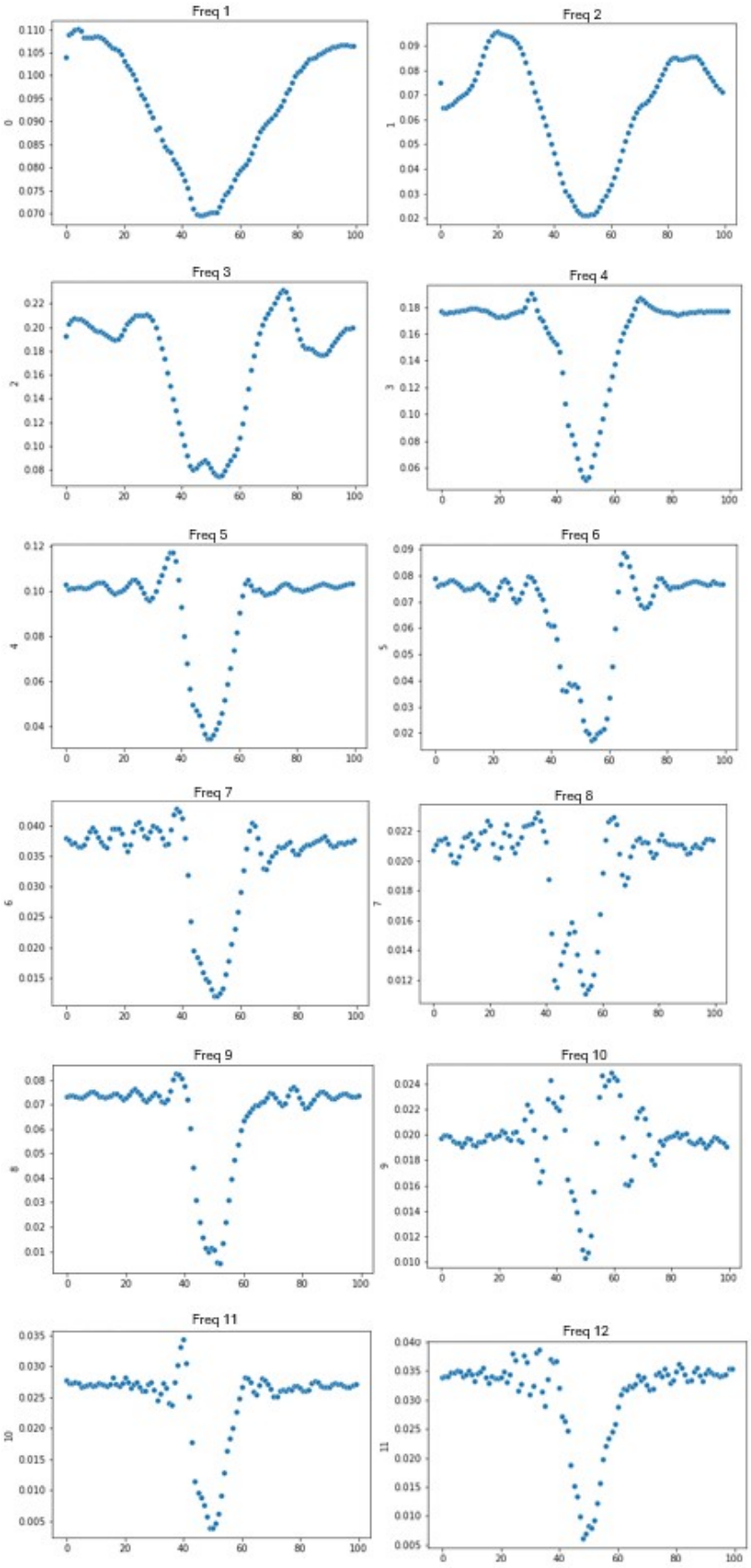

FIGURE 5. 12 individual phases.

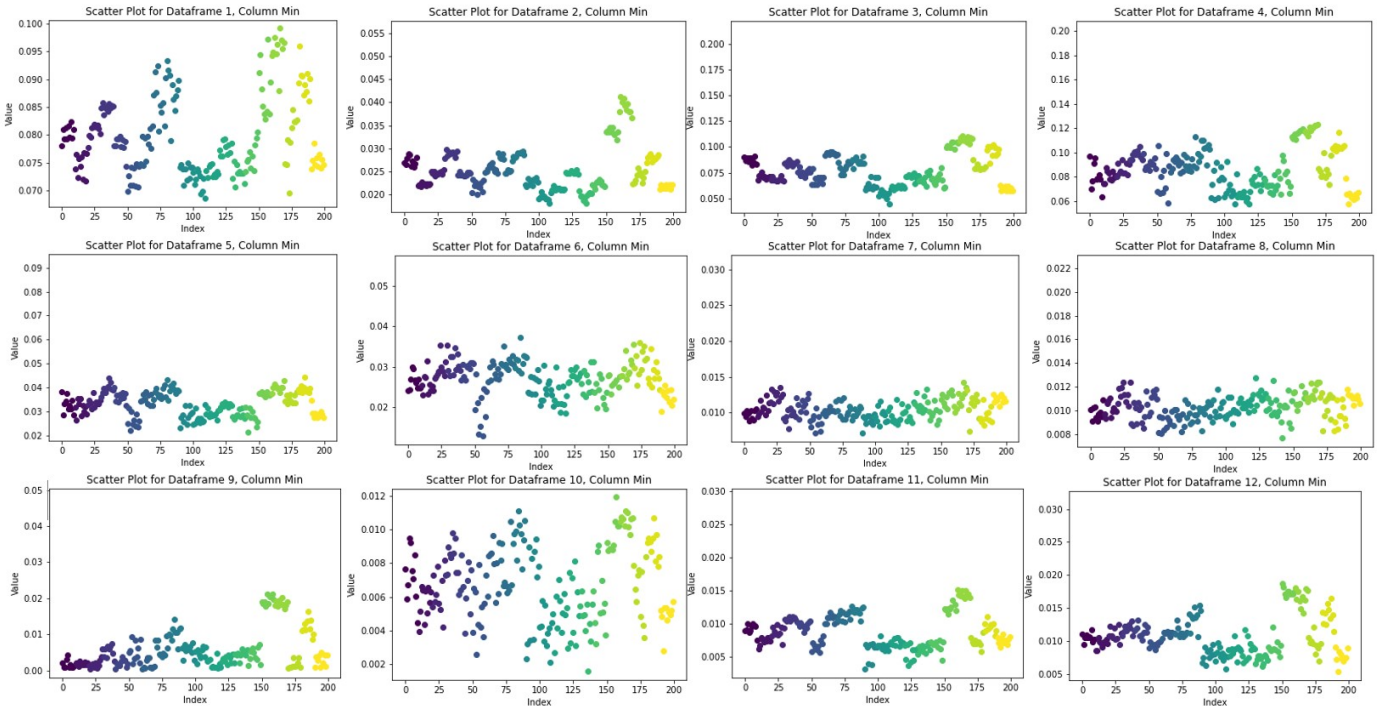

FIGURE 6. Minimum features of 12 discrete frequencies.

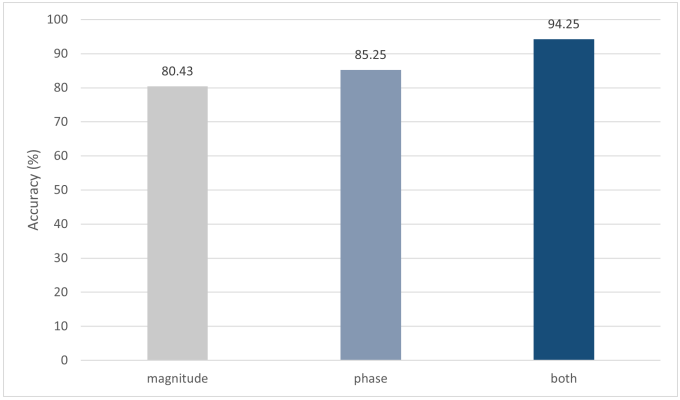

FIGURE 7. Comparison of identification accuracy using magnitude and phase data.

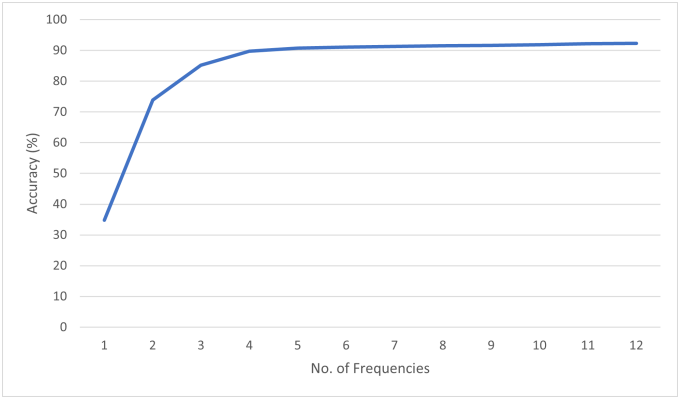

FIGURE 8. Effect of number of frequencies.

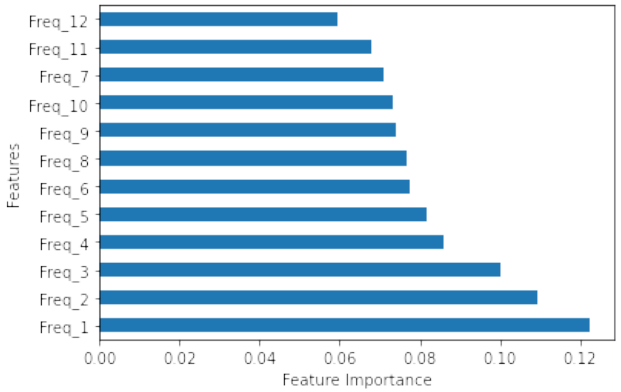

FIGURE 9. Feature Importance vs Frequency.

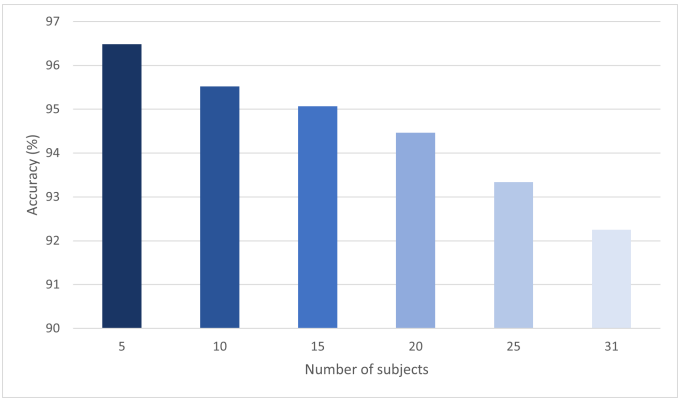

FIGURE 10. Effect of group size on accuracy.

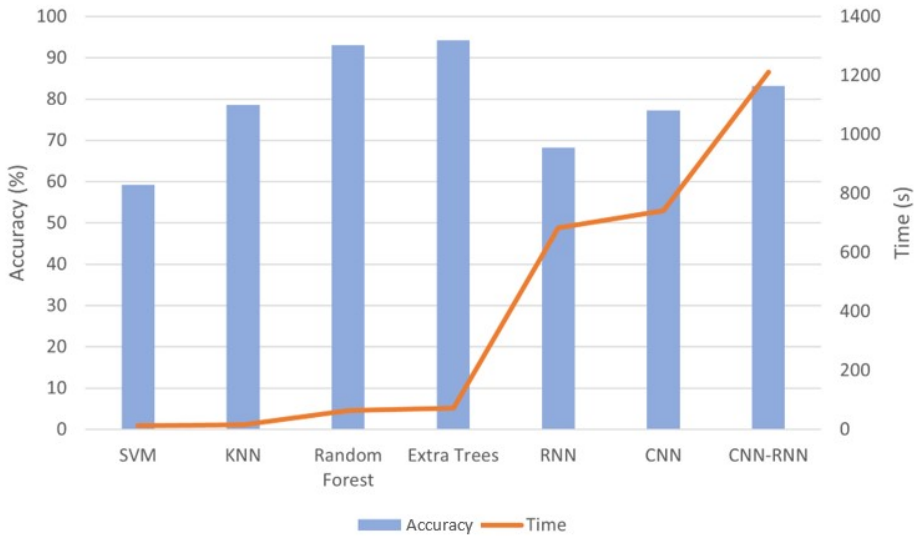

FIGURE 11. Comparison of accuracy and processing time.

in Figure 11. The accuracy rates of each model are represented by the blue bar chart, and their corresponding values are on the vertical axis on the left. These results show that ensemble learning models perform best with random forest achieving 93.1% and extra trees achieving 94.25%. This is followed by the CNN-RNN model at 83.17%. The other four machine learning models examined here have archived accuracy rates below 80%. This is expected based on [5] which showed that random forest outperformed the neural network based models and KNN.

Subsequently, we have evaluated the performance of these models in terms of processing time. The results are represented by the orange coloured line in the chart of Figure 11 and correspond to the values on the vertical axis on the right. It can be observed that the CNN-RNN model requires 15.3 times of the processing time taken for the extra trees model to process at 1211.1 s versus 79.1 s. The KNN and SVM required only a fraction of the processing time of extra trees; however, these models have produced less-than-ideal performances in terms of accuracy.

The precision-recall-iso F1 curve is as shown in Figure 12. The micro-averaged identification performance in terms of precision and recall is 0.93. The average precision (AP) for all participants is above 0.8, except participant number 9 with an average precision of 0.76. Despite the slight decrease in result from participant 9, these results indicate that the system is able to correctly identify participants while maintaining a relatively low rate of false positives.

4.5. Comparison with Related Work

A summary of related works is provided in Table 4. Systems [6, 7, 14, 10] utilize bi-static-like setups for their transmitting and receiving antennas, while systems [14] and [15] utilize a mono-static setup. Our results show that our near-field bi-static radar is capable of producing results on par with that of mono-static systems which have been a more common choice.

TABLE 4. Summary of related work.

System	Sample Size	Signal Type	ML Model	Accuracy (%)
Wihi [6]	8	WiFi	RNN	91
Gate-ID [7]	20	WiFi	RNN	75.7
[14]	7	Radar	CNN-RNN	90
mID [1]	12	Radar	CNN-LSTM	89
RFree-ID [10]	30	Passive RFID	WMD-DTW	92.7
RFPass [15]	20	Passive RFID	CNN-RNN	91.2
Ours	31	RF	Extra Trees	94.25

As evidenced from our investigation in Subsection 4.2 which examines the effect of sample size, systems with smaller sample sizes are generally expected to yield higher accuracy rates than those with larger sample sizes. However, as shown in Table 4, our system with the largest sample size of 31 participants achieves the highest accuracy rate outperforming those with smaller sample sizes ranging from 8 to 20, and RFree-ID [10] with a close sample size of 30 participants.

The confusion matrix in related work records a tendency of lower true positive rates (TPR) among participants with similar physical attributes such as height and weight. Gate-ID [7] records values as low as 0.33 for such instances. Conversely, Wihi [6], which involves participants of similar age but with more varied height and weight, does not exhibit this pattern of discrepancy in its confusion matrix. In contrast, as shown in Figure 13, our system consistently achieves TPRs above 0.80 across all participants, with the majority exceeding 0.9, even among those with closely matching physical attributes.

The prevailing trend in related work favors deep learning; however, our findings suggest that ensemble learning models offer better performance for our dataset. In theory, the com-

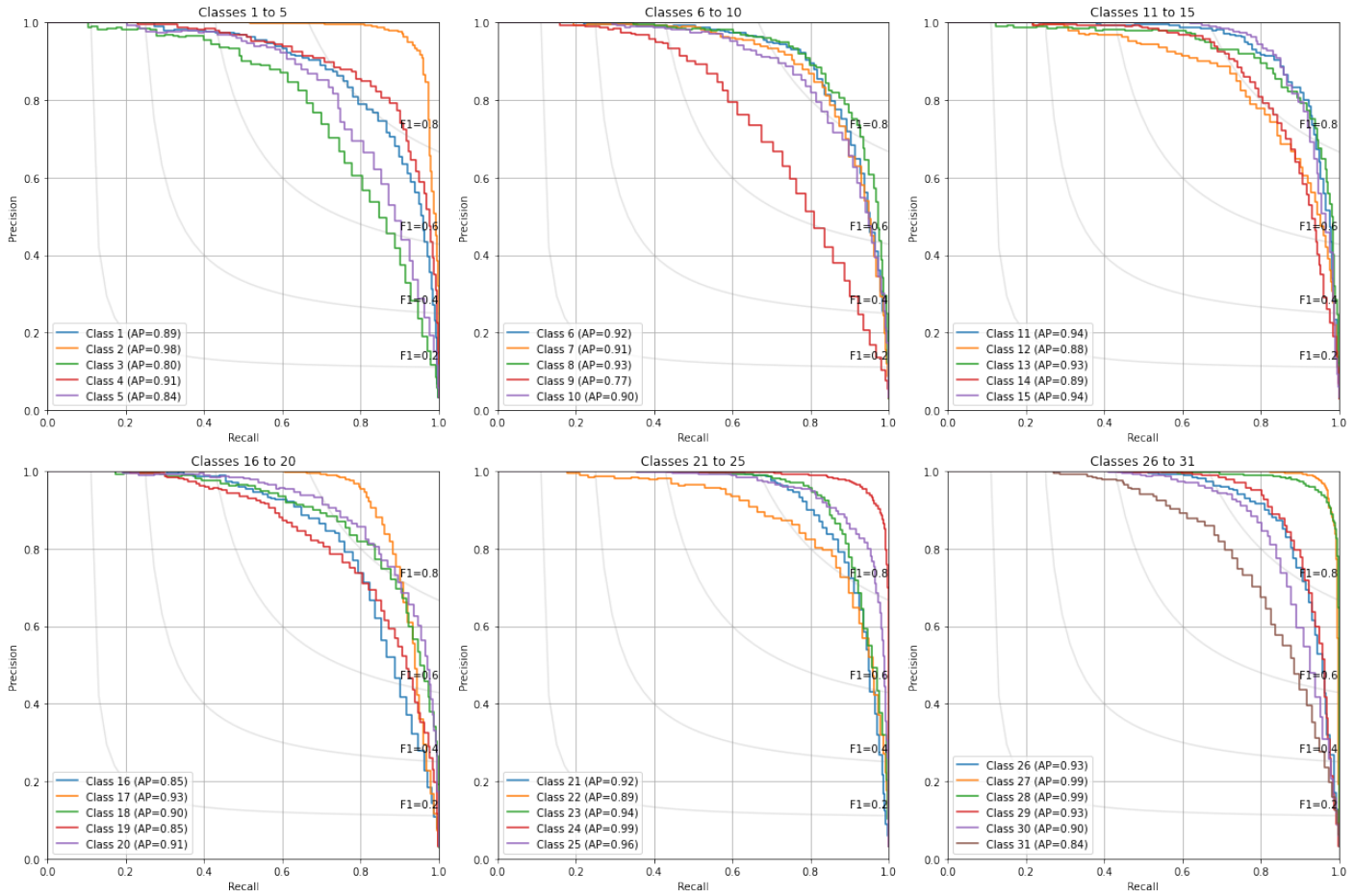

FIGURE 12. PR-isoF1 curve of 31 participants.

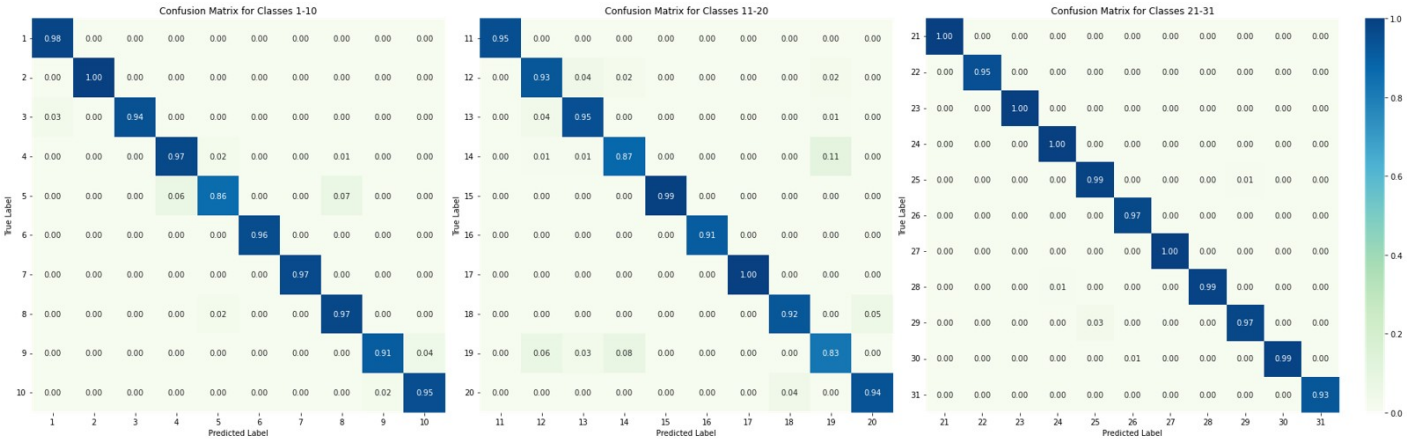

FIGURE 13. Confusion matrix of 31 participants.

plexities of deep learning models should perform better than simple ensemble learning models. Based on the work in [17], we would expect that this is because neural networks have a tendency to overly smooth tabular data, and therefore struggle to create best-fit functions. Our results indicate that this form of data acquisition is more robust and does not require as much machine learning processing to obtain good results.

Taking the varied sample size, signal types, and machine learning models of these systems into consideration, our proposed system has shown to outperform the systems listed here. This shows that our novel method of sensing using near-field bi-static radar, operating on discrete swept frequencies is effective and efficient. However, it is worth noting that the processing times of these approaches are not explicitly provided in the literature, precluding a direct comparison in this regard.

5. CONCLUSION

In this study, we have demonstrated the potential for a novel privacy-preserving human identification utilizing a bi-static radar-like sensor, with signals generated from a discrete frequency sweep. We have examined the effects of various parameters on the performance of our system and found that the usage of both magnitude and phase information provides better coverage for feature extraction. We also conclude that lower frequencies from 50 MHz to 130 MHz provide a higher contribution of informative features than those from 440 MHz to 920 MHz. Therefore, it is not necessary to use more frequencies for higher rates of identification accuracy.

While deep learning is widely used in this area of research, we find that ensemble machine learning works best on our dataset. Specifically, our extra trees model achieves an accuracy of 94.25% with a processing time of 79.1 s.

REFERENCES

[1] Fioranelli, F., M. Ritchie, and H. Griffiths, "Bistatic human micro-Doppler signatures for classification of indoor activities," in *2017 IEEE Radar Conference (RadarConf)*, 0610–0615, 2017.

[2] Zhao, P., C. X. Lu, J. Wang, C. Chen, W. Wang, N. Trigoni, and A. Markham, "Human tracking and identification through a millimeter wave radar," *Ad Hoc Networks*, Vol. 116, 102475, 2021.

[3] Vandersmissen, B., N. Knudde, A. Jalalvand, I. Couckuyt, A. Bourdoux, W. D. Neve, and T. Dhaene, "Indoor person identification using a low-power FMCW radar," *IEEE Transactions on Geoscience and Remote Sensing*, Vol. 56, No. 7, 3941–3952, 2018.

[4] Qiao, X., T. Shan, and R. Tao, "Human identification based on radar micro-Doppler signatures separation," *Electronics Letters*, Vol. 56, No. 4, 195–196, 2020.

[5] Yang, Y., C. Hou, Y. Lang, G. Yue, Y. He, and W. Xiang, "Person identification using micro-Doppler signatures of human motions and UWB radar," *IEEE Microwave and Wireless Components Letters*, Vol. 29, No. 5, 366–368, 2019.

[6] Mokhtari, G., Q. Zhang, C. Hargrave, and J. C. Ralston, "Non-wearable UWB sensor for human identification in smart home," *IEEE Sensors Journal*, Vol. 17, No. 11, 3332–3340, 2017.

[7] Ding, J., Y. Wang, and X. Fu, "Wihi: WiFi based human identity identification using deep learning," *IEEE Access*, Vol. 8, 129 246–129 262, 2020.

[8] Zhang, J., B. Wei, F. Wu, L. Dong, W. Hu, S. S. Kanhere, C. Luo, S. Yu, and J. Cheng, "Gate-ID: WiFi-based human identification irrespective of walking directions in smart home," *IEEE Internet of Things Journal*, Vol. 8, No. 9, 7610–7624, 2021.

[9] Deng, L., J. Yang, S. Yuan, H. Zou, C. X. Lu, and L. Xie, "GaitFi: Robust device-free human identification via WiFi and vision multimodal learning," *IEEE Internet of Things Journal*, Vol. 10, No. 1, 625–636, 2023.

[10] He, Y., Y. Chen, Y. Hu, and B. Zeng, "WiFi vision: Sensing, recognition, and detection with commodity MIMO-OFDM WiFi," *IEEE Internet of Things Journal*, Vol. 7, No. 9, 8296–8317, 2020.

[11] Zhang, Q., D. Li, R. Zhao, D. Wang, Y. Deng, and B. Chen, "RFree-ID: An unobtrusive human identification system irrespective of walking cofactors using cots RFID," in *2018 IEEE International Conference on Pervasive Computing and Communications (PerCom)*, 1–10, Athens, Greece, Mar. 2018.

[12] Chen, Y., J. Yu, L. Kong, Y. Zhu, and F. Tang, "Sensing human gait for environment-independent user authentication using commodity RFID devices," *IEEE Transactions on Mobile Computing*, Vol. 23, No. 5, 6304–6317, 2024.

[13] Dong, S., W. Xia, Y. Li, Q. Zhang, and D. Tu, "Radar-based human identification using deep neural network for long-term stability," *IET Radar, Sonar & Navigation*, Vol. 14, No. 10, 1521–1527, 2020.

[14] Teoh, C. S. and G. A. Ellis, "System and method for detecting, monitoring and identifying human beings," Google Patent, US11074439B2, 2021.

[15] Cleveland, R. and J. Ulcek, "Evaluating compliance with FCC guidelines for human exposure to radiofrequency electromagnetic fields," Federal Communications Commission Office of Engineering and Technology, 1997.

[16] Sharma, A., D. Mishra, T. Zia, and A. Seneviratne, "A novel approach to channel profiling using the frequency selectiveness of WiFi CSI samples," in *GLOBECOM 2020 — 2020 IEEE Global Communications Conference*, 1–6, Taipei, Taiwan, Dec. 2020.

[17] Grinsztajn, L., E. Oyallon, and G. Varoquaux, "Why do tree-based models still outperform deep learning on typical tabular data?" *ArXiv:2207.08815v1*, 2022.